

Synergistic Learning of Lung Lobe Segmentation and Hierarchical Multi-Instance Classification for Automated Severity Assessment of COVID-19 in CT Images

Kelei He, Wei Zhao, Xingzhi Xie, Wen Ji, Mingxia Liu, Zhenyu Tang, Feng Shi, Yang Gao
Jun Liu, Junfeng Zhang and Dinggang Shen, *Fellow, IEEE*

Abstract—Understanding chest CT imaging of the coronavirus disease 2019 (COVID-19) will help detect infections early and assess the disease progression. Especially, automated severity assessment of COVID-19 in CT images plays an essential role in identifying cases that are in great need of intensive clinical care. However, it is often challenging to accurately assess the severity of this disease in CT images, due to small infection regions in the lungs, similar imaging biomarkers, and large inter-case variations. To this end, we propose a synergistic learning framework for automated severity assessment of COVID-19 in 3D CT images, by jointly performing lung lobe segmentation and multi-instance classification. Considering that only a few infection regions in a CT image are related to the severity assessment, we first represent each input image by a bag that contains a set of 2D image patches (with each one cropped from a specific slice). A multi-task multi-instance deep network (called M^2UNet) is then developed to assess the severity of COVID-19 patients and segment the lung lobe simultaneously. Our M^2UNet consists of a patch-

level encoder, a segmentation sub-network for lung lobe segmentation, and a classification sub-network for severity assessment (with a unique hierarchical multi-instance learning strategy). Here, the context information provided by segmentation can be implicitly employed to improve the performance of severity assessment. Extensive experiments were performed on a real COVID-19 CT image dataset consisting of 666 chest CT images, with results suggesting the effectiveness of our proposed method compared to several state-of-the-art methods.

Index Terms—COVID-19, CT, Severity Assessment, Lung lobe Segmentation, Multi-Instance Learning

I. INTRODUCTION

THE coronavirus disease 2019 (COVID-19) is spreading fast worldwide since the end of 2019. Until April 5, about 1.03 million patients are confirmed with this infectious disease, reported by [1]. This raises a Public Health Emergency of International Concern (PHEIC) of WHO. In the field of medical image analysis, many imaging-based artificial intelligence methods have been developed to help fight against this disease, including automated diagnosis [2]–[4], segmentation [5]–[7], and follow-up and prognosis [8].

Previous imaging-based studies mainly focuses on identifying COVID-19 patients from non-COVID-19 subjects. As the golden standard for COVID-19 is the Reverse Transcription-Polymerase Chain Reaction (RT-PCR) test, the effectiveness of this application is limited. Moreover, approximately 80% of patients with COVID-19 have only mild to moderate symptoms [9], while the remaining patients have severe symptoms. Based on our previous studies, the imaging-based characters of COVID-19 patients. Therefore, severity assessment of the disease is of high clinical value, which helps effectively allocate medical resources such as ventilator. Among various radiological examinations, chest CT imaging plays an essential role in fighting this infectious disease by helping early identify lung infections and assess the severity of the disease.

However, automatically assess the severity of COVID-19 in CT images is a very challenging task. First, infections caused by COVID-19 often occur in small regions of the lungs and are difficult to identify in CT images, as shown in Fig. 1. Second, imaging biomarkers of COVID-19 patients caused by infection

This work is supported in part by Key Emergency Project of Pneumonia Epidemic of novel coronavirus infection under grant 2020sk3006, Emergency Project of Prevention and Control for COVID-19 of Central South University under grant 160260005, Foundation of Changsha Scientific and Technical Bureau under grant kq2001001, and National Key Research and Development Program of China under grant 2018YFC0116400. Corresponding authors: Jun Liu (junliu123@csu.edu.cn); Junfeng Zhang (jfzhang@nju.edu.cn); Dinggang Shen (Dinggang.Shen@gmail.com).

K. He and W. Zhao contributed equally to this work.

K. He and J. Zhang are with Medical School of Nanjing University, Nanjing, China. K. He, Y. Gao and J. Zhang are also with the National Institute of Healthcare Data Science at Nanjing University, China (e-mail: hkl@nju.edu.cn).

W. Zhao, X. Xie and J. Liu are with the Department of Radiology, the Second Xiangya Hospital, Central South University, Changsha, Hunan, China. J. Liu is also with the Department of Radiology Quality Control Center, Changsha, Hunan, China (e-mail: wei.zhao@csu.edu.cn; xingzhixie123@csu.edu.cn).

W. Ji and Y. Gao are with State Key Laboratory for Novel Software Technology, Nanjing University, Nanjing, China (e-mail: jiwen@smail.nju.edu.cn; gaoy@nju.edu.cn).

M. Liu is with Biomedical Research Imaging Center and the Department of Radiology, University of North Carolina, Chapel Hill, NC, U.S. (e-mail: mxliu@med.unc.edu).

Z. Tang is with Beijing Advanced Innovation Center for Big Data and Brain Computing, Beihang University, Beijing, China (e-mail: tangzhenyu@buaa.edu.cn).

F. Shi and D. Shen are with the Department of Research and Development, Shanghai United Imaging Intelligence Co., Ltd., Shanghai 200232, China (e-mail: feng.shi@united-imaging.com).

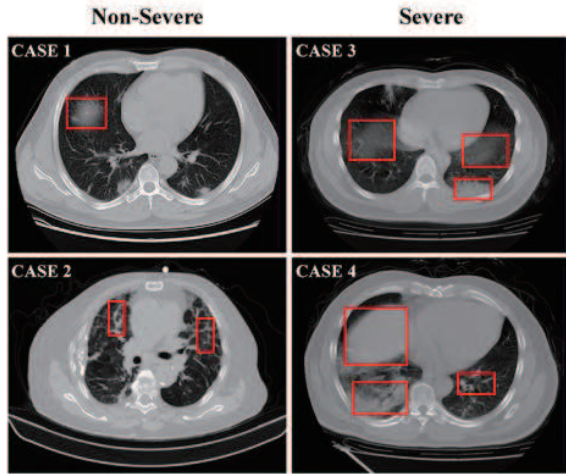


Fig. 1. Typical cases of two non-severe (left) and two severe (right) patients with COVID-19, where infections often occur in small regions of the lungs in CT images. The similar imaging biomarkers (e.g., ground glass opacities, mosaic sign, air bronchogram and interlobular septal thickening) of both cases (denoted by red boxes) make the non-severe and severe images difficult to distinguish.

in some severe and non-severe cases are similar, including ground glass opacities (GGO), mosaic sign, air bronchogram and interlobular septal thickening (see Fig. 1). In addition, there are large inter-case variations in CT images of COVID-19 patients (see Fig. 2), because these images are usually acquired by multiple imaging centers with different scanners and different scanning parameters.

Several recent methods have been proposed for the diagnosis of COVID-19 [2]–[4], with only some specifically designed for severity assessment of the disease. In several studies [5]–[7], segmentation of lung or lung lobe is used as a pre-requisite procedure for diagnosis purposes. However, most of these methods treat the lung lobe segmentation and the disease diagnosis as two separate tasks, ignoring their underlying association. Note that the segmentation of lung lobe can provide rich information regarding spatial locations and tissue types in CT images. Therefore, it is intuitively reasonable to jointly perform lung lobe segmentation and severity assessment/prediction, where the context information provided by segmentation results can be used to improve the prediction performance. Besides, as demonstrated by related works of class activation maps (CAMs) [10], the classification task can raise high signal responses in lung lobe area, which can also provide useful guidance for the segmentation of lung lobes. Moreover, most of the previous works are based on 2D image slices [2]–[4], so the spatial structural information of CT images is ignored. It is interesting to directly employ 3D CT images for automated severity assessment of COVID-19, which is desired for real-world clinical applications.

To this end, in this paper, we propose a synergistic learning framework for automated severity assessment of COVID-19 in 3D CT images, by jointly performing severity assessment of COVID-19 patients and lung lobe segmentation. Specifically, we represent each input CT image by a bag that contains a set of randomly cropped 2D image patches (with each patch corresponding to a specific slice), considering that only a

few infection regions in CT images are related to severity assessment. With each bag as input, a multi-task multi-instance deep neural network (called M²UNet) is developed, including a shared patch-level encoder, a segmentation sub-network for lung lobe segmentation, and a classification sub-network for severity assessment of COVID-19 patients (i.e., severe or non-severe) using a hierarchical multi-instance learning strategy. Here, the segmentation results are used to provide context information of input CT images to boost the performance of severity assessment. Extensive experiments have been performed on a real-world COVID-19 dataset with 666 chest CT images, with results demonstrating the effectiveness of the proposed method compared to several state-of-the-art methods.

The contributions of this work are three-fold:

- A multi-task multi-instance learning framework is proposed to jointly assess the severity of the COVID-19 patients and segment the lung lobe in chest CT images, where the segmentation task provides context information to aid the task of severity assessment in chest CT images.
- A unique hierarchical multi-instance learning strategy is developed to predict the severity of patients in a weakly supervised manner.
- We evaluate the proposed method on a real clinical dataset with 666 3D CT images of COVID-19 patients, achieving promising results in severity assessment compared to several state-of-the-art methods.

The rest of the paper is organized as follows. In Section II, we introduce the related works for the segmentation and diagnosis of CT images of COVID-19 patients, as well as related studies on deep multiple instance learning. We then introduce the proposed method in Section III. In Section IV, we present the materials, experimental setup, and experimental results. We finally conclude this paper and present several future research directions in Section V.

II. RELATED WORKS

In this section, we briefly review the most relevant studies from the following three aspects: 1) lung segmentation of CT images with COVID-19, 2) automated diagnosis of COVID-19 patients, and 3) deep multi-instance learning.

A. Lung Segmentation of CT Images with COVID-19

Segmentation of lung or lung lobe has been used as a common pre-requisite procedure for automatic diagnosis of COVID-19 based on chest CT images. Several deep learning methods have been proposed for lung segmentation of CT images with COVID-19. For instance, U-Net *et al.* [11] has been widely used for segmentation of both lung regions and lung lesions in COVID-19 applications [7], [12]–[14]. Qi *et al.* [7] use U-Net to delineate the lesions in the lung and extract radiomics features of COVID-19 patients with the initial seeds given by a radiologist for predicting hospital stay. And several variants of U-Net have been applied to the diagnosis or severity assessment of COVID-19. Jin *et al.* [6] design a two-stage pipeline to screen COVID-19 in CT images, and they utilize U-Net++ [15] to detect the whole lung region

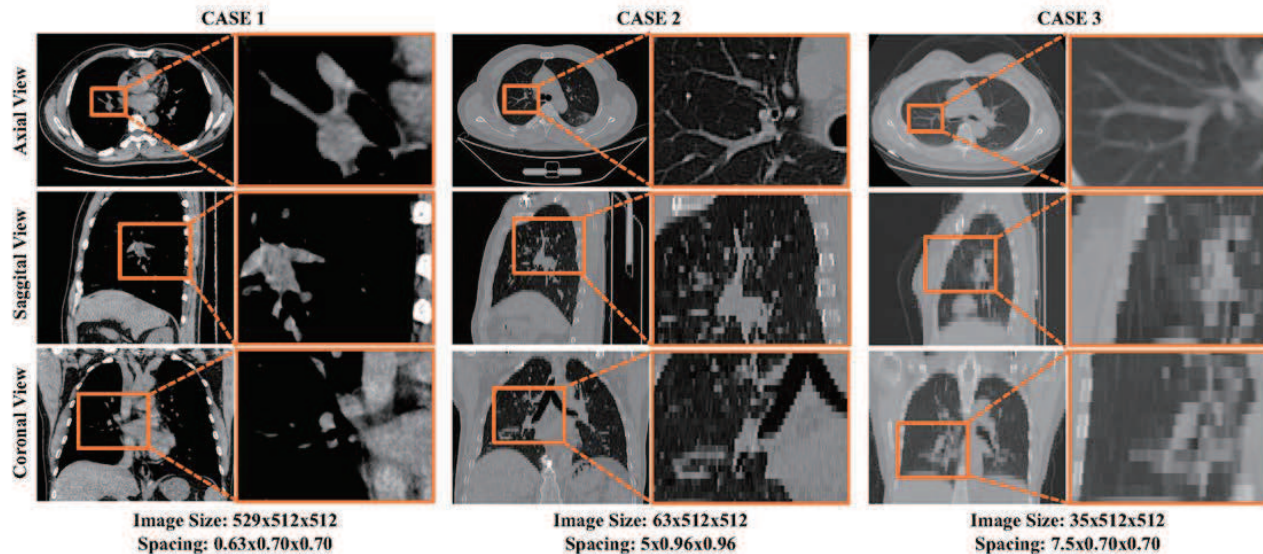


Fig. 2. Visualization of three typical cases in the COVID-19 CT image dataset from three different views. As shown in this figure, large inter-case variations (e.g., image size and spatial resolution) exist in CT images of COVID-19 patients.

and to separate the lesions from lung regions. Besides, V-Net [16] is also used in various segmentation applications. Shan *et al.* [5] integrate human-in-the-loop strategy into the training process of VB-Net (a variant of V-Net). The human-aided strategy is a intuitive way to address the deficiency of labels for segmentation of COVID-19 in CT images.

B. Automated Diagnosis of COVID-19

Both X-rays and CT images can provide effective information for computer-assisted diagnosis of COVID-19. Compared with X-rays, chest CT imaging contains hundreds of slices, which is clearer and more precise but has to take more time for the specialists to diagnose. Therefore, there is a great demand to use CT images for automated diagnosis of COVID-19. In general, existing methods for COVID-19 diagnosis based on CT images can be roughly divided into two categories: 1) classification; 2) severity assessment. In the former category, many studies have been conducted to determine whether patients are infected with the COVID-19 disease. For example, Chen *et al.* [2] exploit a UNet++ based segmentation model to segment COVID-19 related lesions in chest CT images of 51 COVID-19 patients and 55 patients with other diseases, and finally determine the label (COVID-19 or non-COVID-19) of each image based on the segmented lesions. Ying *et al.* [3] propose a CT diagnosis system, namely DeepPneumonia, which is based on ResNet50 model to identify patients with COVID-19 from bacteria pneumonia patients and healthy people. In the second category, Tang *et al.* [4] proposed to first adopt VB-Net to separate the lung into anatomical sub-regions, and then use these sub-regions as quantitative features to train a random forest (RF) model for COVID-19 severity assessment (with labels of being non-severe or severe).

C. Deep Multi-Instance Learning

The scenario of multi-instance learning (MIL) [17]–[19] or learning from weakly annotated data [20] arises when only

a general statement of the category is given, but multiple instances can be observed. MIL aims to learn a model which can predict the label of a bag accurately, and many recent studies have focused on implementing MIL via deep neural networks. For instance, Oquab *et al.* [20] train a deep model with multiple image patches of multiple scales as input, and aggregate the prediction results of multiple inputs by using a max pooling operation. Besides, many studies [21]–[23] propose to formulate image classification as a MIL problem so as to address the weakly supervised problem. Moreover, MIL is particularly suitable for problems with only a limited number (e.g., tens or hundreds) of training samples in various medical image based applications, such as computer-assisted disease diagnosis [24]–[27]. For instance, Yan *et al.* [26] propose a two-stage deep MIL method to find discriminative local anatomies, where the first-stage convolutional neural network (CNN) is learned in a MIL fashion to locate discriminative image patches and the second-stage CNN is boosted using those selected patches. More recently, a landmark-based deep MIL framework [27] is developed to learn both local and global representations of MRI for automated brain disease diagnosis, leading to a new direction for handling limited training samples in the domain of medical image analysis. Since there are only a limited number of cases at hand, it is desirable to employ the multi-instance learning strategy for severity assessment of COVID-19 patients in chest CT images.

III. PROPOSED METHOD

A. Framework

The framework of the proposed method is illustrated in Fig. 3, where the input is the raw 3D CT image and the output is the lung segmentation and severity assessment of COVID-19 patients (i.e., severe or non-severe). Specifically, each 3D CT image is processed via several image pre-processing steps. Then, a set of 2D image patches is randomly cropped from the processed image to construct an instance bag, and each bag

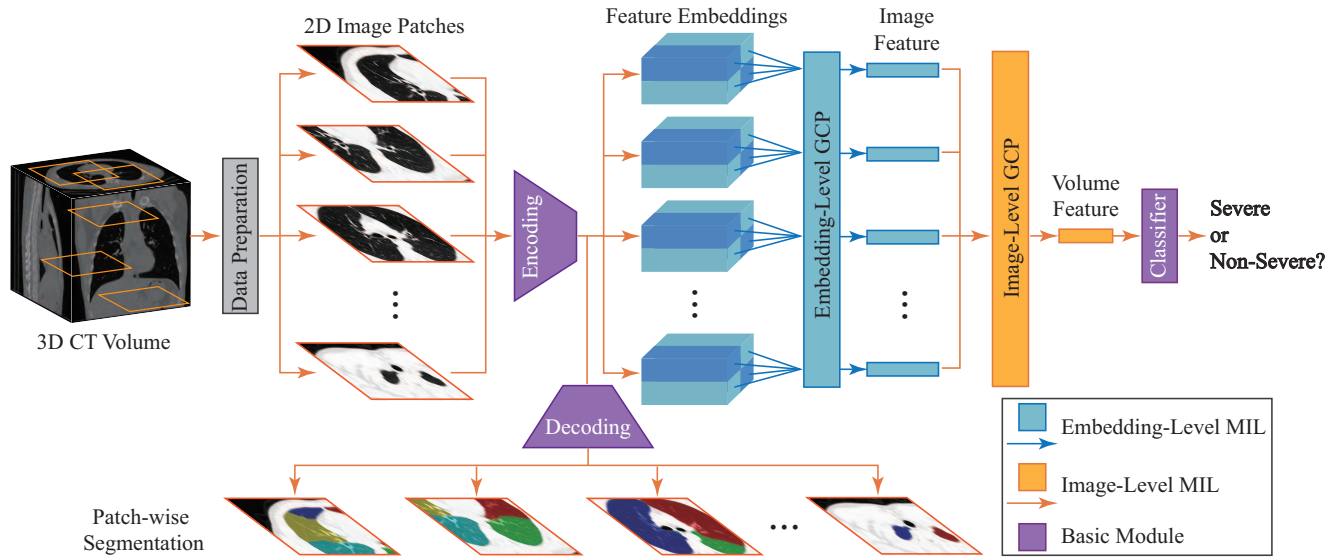


Fig. 3. Illustration of the proposed framework for joint lung lobe segmentation and severity assessment of COVID-19 in 3D CT images. Each raw 3D CT image is first pre-processed, and multiple 2D image patches (with each patch corresponding to a specific slice) are then extracted to construct an instance bag for representing each input CT scan. This bag is then fed into the proposed multi-task multi-instance UNet (M^2UNet) for jointly lung lobe segmentation and severity assessment of COVID-19, consisting of a shared patch-level encoder, a segmentation sub-network, and a classification sub-network for severity assessment. Here, the segmentation task can provide location and tissue guidance for the task of severity assessment that employs a hierarchical multi-instance learning strategy.

represents a specific input CT image. This bag is regarded as the input of the proposed multi-task multi-instance UNet (M^2UNet). The M^2UNet is designed to learn two tasks jointly, i.e., severity assessment of a COVID-19 patient and segmentation of the lung lobe.

As shown in Fig. 3, in M^2UNet , an encoding module is first used for patch-level feature extraction of 2D patches in each input bag, followed by two sub-networks for joint severity assessment and lung lobe segmentation. Specifically, in the classification sub-network, these extracted patch-level features are fed into a feature embedding module and an image-level feature learning module to capture the local-to-global volume representation of the input CT image. With the learned volume features, a classification layer is finally used to assess the severity of each COVID-19 patient (i.e., severe or non-severe). In the segmentation sub-network, those patch-level features are fed into a decoding module to perform lung lobe segmentation for each patch in the input bag. Since these two sub-networks are trained jointly with a shared patch-level encoder, the context information provided by the segmentation results can be implicitly employed to improve the performance of severity assessment.

B. Data Preparation

To eliminate the effect of the background noise in each raw 3D CT image, we crop each scan to only keep the region containing the human body, by using a threshold-based processing method. Specifically, we first binarize the image using the threshold of zero, through which the human tissues and the gas regions will be separated. Then, the human body region is cropped according to the binary mask. Each body

region image has the size of at least 256×256 for the axial plane in this work.

While image resampling is commonly used in many deep learning methods for segmentation and classification [28], [29], we do not resample the raw CT images in order to preserve their original data distributions. Since our method is clinical-oriented with inconsistent imaging qualities, CT images used in this study are not as clean as those in benchmark datasets [30]. For example, the physical spacing of our data has large variation, e.g., from 0.6 mm to 10 mm between slices, because of the use of different CT scanners and scanning parameters. Using a common interpolation method (e.g., tri-linear interpolation) to resample a CT image into 1 mm , one will introduce heavy artifacts to the image. Besides, only a few infection regions in each CT image are related to severity assessment. To this end, we employ the weakly supervised multi-instance learning (MIL) strategy for handling these inconsistent CT images. Specifically, for each pre-processed CT image, we randomly crop a set of 2D patches sampled from 2D slices (with each patch from a specific slice) in each image to construct an instance bag, and each bag is used to represent a specific CT image and treated as the input of the subsequent M^2UNet . In this way, the inter-slice/patch relationships can be implicitly captured by our M^2UNet . In addition, this MIL strategy represents each 3D image through a set of 2D image patches rather than sequential slices. This can partially alleviate the problem of data inconsistency, so our method has high practical value in real-world applications.

C. Network Architecture

As shown in Fig. 3, using each bag (consisting of a set of 2D image patches) as the input data, the proposed M^2UNet first

employ an encoding module for patch-level feature extraction. Based on these features, a classification and a segmentation sub-networks are then used to jointly perform two tasks, respectively, i.e., 1) severity assessment of the patients, and 2) segmentation of lung lobes in each patch. Specifically, the classification sub-network uses a unique hierarchical MIL strategy to extract the local-to-global representation of each input image, with a embedding-level MIL module, an image-level MIL module, and a classification module. The segmentation sub-network contains a decoding module to segment lung lobes of 2D image patches in each bag.

The detailed network architecture is listed in Table I. The combination of the encoder and decoder is U-Net like, with four down-sampling blocks in the encoder and four up-sampling blocks in the decoder. The outputs of the same level blocks in the encoder and decoder are concatenated and fed into the next block of the decoder. Limited by computational resources, all the convolutional layers in the encoder and decoder have the same number (i.e., 64) of kernels, except the last block in the encoder. The last block of encoder outputs 512 dimensional features to help build a more robust classification for severity assessment. The decoder outputs the corresponding segmentation mask of six types of lung lobes for each image patch.

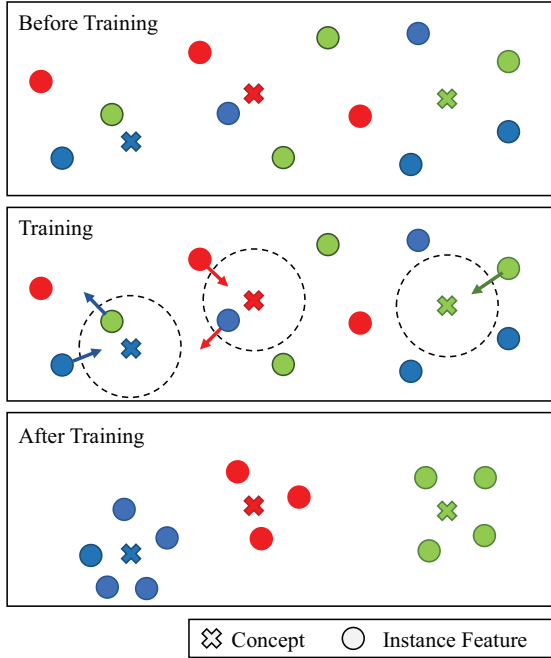


Fig. 4. A brief illustration of the learning principle for the proposed global contrast pooling (GCP) layer. Here, the concepts denote to-be-learned features that are discriminative for severity assessment. The GCP layer is designed to pull the relevant instance feature and concept closer, and push the irrelevant instance feature and concept away from each other.

D. Hierarchical Multi-Instance Learning

While infection regions of the lung that related to COVID-19 (e.g., nodule and GGO) are usually located in small regions of the CT image, the category of each CT image is labeled

at the entire image level, rather than the region level. That is, many regions are actually unrelated to the classification task for severity assessment. Multi-instance learning (MIL) provides a useful tool to solve such a weakly supervised problem. Conventional MIL represents a 2D image as a bag, and each bag consists of multiple instances (i.e., regions of the input image). The prediction is done on the bag-level by learning the relationship among instances in embedding-level MIL methods, or just by performing voting on the instance predictions in instance-level methods. However, these methods are not applicable for the classification of 3D images, as 3D images contain multiple 2D image slices. In this work, based on the previous study on pathological images [], we propose a hierarchical MIL strategy in the classification sub-network of our M²UNet to perform severity assessment of COVID-19 in 3D CT images, as shown in Fig. 3.

As mentioned in Section III-B, we represent each input 3D volumetric image as a bag consisting of a set of 2D image patches, and these patches are regarded as the instances in the MIL problem settings. Formally, we first construct a bag with n 2D patches cropped from the body regional slices to represent each input CT image. Denote the i -th and the j -th 3D CT image as \mathcal{X}_i and \mathcal{X}_j , respectively, where $\mathcal{X}_i = \{\phi_{i1}^{ins}, \phi_{i2}^{ins}, \dots, \phi_{in_i}^{ins}\}$ and $\mathcal{X}_j = \{\phi_{j1}^{ins}, \phi_{j2}^{ins}, \dots, \phi_{jn_j}^{ins}\}$. Here, $\phi_{kl}^{ins} \in \mathbb{R}^d$ ($k = 1, 2, \dots, n_k$) indicates the l -th instance of the k -th image. Then, these 2D patches (size: $height \times width$) are fed into the encoding module for patch/instance-level feature extraction. These instance-level feature is further fed into an embedding-level MIL module, which will be introduced later. After obtaining the instance-level features, the bag/image-level feature Φ_i are then generated by our proposed global contrast pooling (GCP) layer in the image-level MIL module.

In this work, we use the term ‘concept’ to denote the to-be-learned feature of GCP layer that is discriminative for severity assessment. As illustrated in Fig. 4, the proposed GCP layer aims to pull the relevant instance features and concepts to be close, and also push those irrelevant instance features and concepts away from each other. Specifically, in the GCP layer, we assume the bag-level feature Φ_i is represented by the relationship between instance features and p concepts. Here, these concepts are learned to reveal the data structure in a global perspective. The bag-level feature is then denoted as a p dimensional feature vector, with each dimension denoting the maximum similarity between one concept and all instance features. We use the cosine function to measure such relationship. Thus, the bag feature and the similarity can be written as

$$\Phi_i = [s_{i1}, s_{i2}, \dots, s_{im}, \dots, s_{ip}], \quad (1)$$

$$s_{im} = \max_{k=1}^{n_i} \mathbf{w}_m^\top \phi_{ik} + \mathbf{R}(\mathbf{w}_m), \quad (2)$$

where s_{im} ($m = 1, \dots, p$) is the maximum similarity between the instance features of the i -th bag and m -th image-level concept w_m . $R(\cdot)$ denotes the regularization term used in deep networks. With Eqs. (1)-(2), one can observe that the proposed GCP layer can automatically learn the concepts

TABLE I

NETWORK ARCHITECTURE OF THE PROPOSED M²UNET. THE NETWORK HAS THREE MAIN COMPONENTS: 1) A ENCODING MODULE CONTAINS FIVE ENCODING BLOCKS; 2) A CLASSIFICATION SUB-NETWORK CONTAINING THE EMBEDDING-LEVEL MIL AND IMAGE-LEVEL MIL, AND A CLASSIFIER; AND 3) A SEGMENTATION SUB-NETWORK CONSISTING OF A DECODING MODULE WITH FIVE DECODING BLOCKS. MIL: MULTI-INSTANCE LEARNING; NUM.: NUMBER OF LAYERS, K: KERNEL SIZE; PAD: PADDING SIZE; STR: STRIDE; #: NUMBER OF LEARNABLE PARAMETERS; COV: CONVOLUTION; GCP: GLOBAL CONTRAST POOLING; CONCAT: CONCATENATION.

Block Name	Num.	Layers	Parameter Setting	Input	#
Encoding block 1	2	{conv, batchnorm, ReLU}	K: {3 × 3 × 64}, PAD:1, STR:1	2D image patches	37K
Pool 1	1	max-pooling	K: {2 × 2}, STR:2	Encoding block 1	—
Encoding block 2	2	{conv, batchnorm, ReLU}	K: {3 × 3 × 64}, PAD:1, STR:1	Pool 1	72K
Pool 2	1	max-pooling	K: {2 × 2}, STR:2	Encoding block 2	—
Encoding block 3	2	{conv, batchnorm, ReLU}	K: {3 × 3 × 64}, PAD:1, STR:1	Pool 2	72K
Pool 3	1	max-pooling	K: {2 × 2}, STR:2	Encoding block 3	—
Encoding block 4	2	{conv, batchnorm, ReLU}	K: {3 × 3 × 64}, PAD:1, STR:1	Pool 3	72K
Pool 4	1	max-pooling	K: {2 × 2}, STR:2	Encoding block 4	—
Encoding block 5	1	{conv, batchnorm, ReLU}	K: {3 × 3 × 64}, PAD:1, STR:1	Pool 4	2595K
	1	{conv, batchnorm, ReLU}	K: {3 × 3 × 512}, PAD:1, STR:1		
Embedding-Level MIL	1	GCP	Num. Concepts: 256	Encoding block 5	193K
	1	conv	K: {1 × 1 × 256}, PAD:0, STR:1		
Image-Level MIL	1	GCP	Num. Concepts: 128	Embedding-Level MIL	48K
	1	conv	K: {1 × 1 × 128}, PAD:0, STR:1		
Classifier	1	conv	K: {1 × 1 × 128}, PAD:0, STR:1	Image-Level MIL	0.3K
Decoding block 5	1	{up-sample, conv, batchnorm, ReLU, concat}	K: {3 × 3 × 512}, PAD:1, STR:1	Encoding block 5	397K
	2	{conv, batchnorm, ReLU}	K: {3 × 3 × 128}, PAD:1, STR:1	Encoding block 4	
Decoding block 4	1	{up-sample, conv, batchnorm, ReLU, concat}	K: {3 × 3 × 64}, PAD:1, STR:1	Decoding block 5	145K
	2	{conv, batchnorm, ReLU}	K: {3 × 3 × 128}, PAD:1, STR:1	Encoding block 3	
Decoding block 3	1	{up-sample, conv, batchnorm, ReLU, concat}	K: {3 × 3 × 64}, PAD:1, STR:1	Decoding block 4	145K
	2	{conv, batchnorm, ReLU}	K: {3 × 3 × 128}, PAD:1, STR:1	Encoding block 2	
Decoding block 2	1	{up-sample, conv, batchnorm, ReLU, concat}	K: {3 × 3 × 64}, PAD:1, STR:1	Decoding block 3	145K
	2	{conv, batchnorm, ReLU}	K: {3 × 3 × 128}, PAD:1, STR:1	Encoding block 1	
Decoding block 1	1	conv	K: {1 × 1 × 64}, PAD:0, STR:1	Decoding block 2	0.5K

that are related to those discriminative instances, thus reducing the influence of those irrelevant instances. Note such a GCP layer can be also used in other weakly supervised problems, where only a small portion of regions in an image are related to the task at hand (such as MRI-based brain disorder diagnosis [27]).

We further use an embedding-level MIL module (with a GCP layer) to learn embedding-level representations, by regarding each image patch as a bag and the intermediate patch-level features produced by the encoder as instances. In this way, the relationships among small regions in each patch can be modeled by our method. Based on the embedding-level features, an image-level MIL module (with a GCP layer) is further used to generate the volume features. Based on the volume features, we use a fully-connected layer followed by a cross-entropy loss to predict the severity score (i.e., severe or non-severe) of each input CT image. The final loss function in the proposed hierarchical MIL network for severity assessment can be formulated as

$$\mathcal{L}_{MIL} = -\log(fc(\Phi_i), y), \quad (3)$$

where $fc(\cdot)$ denotes the mapping function of the fully-connected layer, and y denotes the severity type confirmed by clinicians.

E. Multi-Task Learning for Joint Lung Segmentation and Severity Assessment

The segmentation task is supervised by the aggregation of cross-entropy loss and Dice loss as follows

$$\mathcal{L}_{seg} = -\frac{1}{N} \sum_{n=1}^N \sum_{c=1}^C \log(\hat{p}_n^c, l_n^c) - 2 \times \frac{\sum (\hat{p}_n^c \cap l_n^c)}{\sum \hat{p}_n^c + \sum l_n^c} + 1, \quad (4)$$

where \hat{p}_n^c and l_n^c denote the predicted and ground-truth segmentation masks for the n -th patch in the c -th category. In this work, we segment $c = 7$ categories, including six parts of lung lobe and the background. It is worth noting that most of the cases in our dataset do not have ground-truth segmentation masks. For these cases, we simply avoid calculating the segmentation loss for them.

Finally, the losses in Eqs. 3 and 4 are trained simultaneously in a multi-task learning manner, and the overall loss of the proposed method is written as

$$\mathcal{L} = \lambda \mathcal{L}_{MIL} + \mathcal{L}_{seg}, \quad (5)$$

where λ is the trade-off parameter used to balance the contributions of these two tasks. In this work, λ is empirically set to 0.01.

F. Implementation

The proposed method is implemented based on the open-source deep learning library *Pytorch*. The training of the network is accelerated by four NVidia Tesla V100 GPUs

TABLE II
QUANTITATIVE COMPARISON FOR SEVERITY ASSESSMENT TASKS WITH THE STATE-OF-THE-ART METHODS.

Method	Accuracy	Precision	Recall	F1 Score	AUC
ResNet50+Max [31]	0.924 \pm 0.497	0.856 \pm 0.154	0.793 \pm 0.106	0.816 \pm 0.120	0.803 \pm 0.090
Gated Att. MIL [32]	0.955 \pm 0.015	0.879 \pm 0.054	0.946 \pm 0.019	0.906 \pm 0.037	0.973 \pm 0.024
Tang <i>et al.</i> [4]*	0.875	-	0.933	-	0.910
Yang <i>et al.</i> [33]	-	-	0.750	-	0.892
Cls. Only (Ours)	0.969 \pm 0.023	0.928 \pm 0.073	0.958 \pm 0.031	0.938 \pm 0.045	0.980 \pm 0.013
M ² UNet (Ours)	0.985 \pm 0.005	0.975 \pm 0.022	0.952 \pm 0.011	0.963 \pm 0.011	0.991 \pm 0.010

TABLE III
QUANTITATIVE COMPARISON FOR THE PERFORMANCE OF LUNG LOBE SEGMENTATION WITH THE STATE-OF-THE-ART METHODS.

Method	# (MB)	DSC	SEN	PPV
U-Net	131.71	0.776 \pm 0.050	0.759 \pm 0.037	0.834 \pm 0.033
U-Net++	34.97	0.784 \pm 0.035	0.773 \pm 0.038	0.821 \pm 0.018
Seg. Only (Ours)	14.37	0.759 \pm 0.055	0.756 \pm 0.064	0.785 \pm 0.045
M ² UNet (Ours)	15.32	0.785 \pm 0.058	0.783 \pm 0.059	0.799 \pm 0.051

(each with 32 GB memory). For feasible learning of the lung region images, we clamp the intensities of the image into $[-1200, 0]$, which indicates that we use the width of 1200 and level of -600 for the pulmonary window. Then, the data is normalized to the value of $[0, 255]$, as used by other deep learning methods. The dataset is highly unbalanced as the number of severe patients is much fewer than the non-severe patient. Therefore, we augmented the data by directly duplicated the severe cases in the training set. This can be done because the proposed method use a random crop strategy to construct the inputs. This makes the duplicated cases not same to each other for the training of the network. We also use the random crop strategy in testing stage, by assuming the data distribution is already well learned in training. Please note that, other cropping strategies, e.g., center cropping, can also be used here. However, the center of pulmonary is dominated by trachea and other tissues, center cropping may not suitable here.

In both training and testing stage, we randomly crop 200 image patches from each input 3D CT image to construct the image-level bag (i.e., with the bag size of $n = 200$). And we use the output of the encoder to construct the embedding-level bag that contains 8×8 feature maps. We train M²UNet using the learning rate of 0.01 with a decay strategy of ‘Poly’ (with power of 0.75). The network is optimized by a standard Stochastic Gradient Descent (SGD) algorithm with 100 epochs. And the weights are decayed by a rate of 1×10^{-4} with the momentum of 0.9.

IV. EXPERIMENTS

In this section, we first introduce the materials, competing methods, and experimental setup. We then present the experimental results achieved by our method and several state-of-the-art methods. We finally investigate the influence of two major strategies used in our method. More results on parameter analysis can be found in the *Supplementary Materials*.

A. Materials

The real COVID-19 dataset contains a total of 666 3D chest CT scans acquired from 242 patients who are confirmed with COVID-19 (i.e., RT-PCR Test Positive). These CT images are collected from seven hospitals with a variety of CT scanners, including Philips (Ingenuity CT iDOSE4), GE (Bright speed S), Siemens (Somatom perspective), Hitachi (ECLoS), and Anke (ANATOM 16HD). The images are of large variation in terms of the image size of $512 \times (512 \sim 666) \times (23 \sim 732)$, and the spatial resolution of $0.586 \sim 0.984 \text{ mm}$, $0.586 \sim 0.984 \text{ mm}$ and $0.399 \sim 10 \text{ mm}$. Obviously, diagnosis based on these images is a very challenging task. The severity of the patients are confirmed by clinicians, following the guideline of 2019-nCoV (trial version 7) issued by the China National Health Commission. The severity of the patients are categorized into four types, i.e., mild, moderate, severe, and critical. In clinical practice, patients are often divided into two groups with different treatment regimen, i.e., severe and non-severe. In this work, we employ this partition strategy. That is, mild and moderate are treated as non-severe, while severe and critical are regarded as severe. Therefore, the task of severe assessment is formulated into a binary classification problem.

B. Competing Methods

We first compare the proposed M²UNet with four state-of-the-art methods in [4], [31]–[33] for severity assessment of COVID-19 patients. The first two methods [4], [33] are both based on hand-crafted features of CT images, while the last two [31], [32] are deep learning-based methods that can learn imaging features automatically from data. Specifically, Tang *et al.* [4] first segment the lung, lung lobe and lesions in CT images. Then, the quantitative features of COVID-19 patients, e.g., the infection volume and the ratio of the whole lung, are calculated based on the segmentation results. The prediction is done by a random forest method. Yang *et al.* [33] propose to aggregate infection scores calculated on 20 lung

regions for severity assessment. Besides, the ResNet50+Max method [31] is also compared for patch-wise classification. ResNet50+Max is a non-MIL method, which has a ResNet-50 network architecture and performs image-level classification through max-voting. In addition, we apply the Gated Att. MIL method proposed in [32] on our dataset, which is a one-stage MIL method with an attention mechanism. For the fair comparison, this method shares the same multiple instance pool as our M²UNet.

We further compare our method with two state-of-the-art methods for lung lobe segmentation, including 1) UNet [11], and 2) UNet++ [15]. The parameter settings for these five competing methods are the same as those in their respective papers.

To evaluate the influence of the proposed multi-task learning and hierarchical MIL strategies used in M²UNet, we further compare M²UNet with its two variants: 1) M²UNet with only the classification sub-network (denoted as Clas. Only), 2) M²UNet with only the segmentation sub-network (denoted as Seg. Only).

C. Experimental Setup

A five-fold cross-validation (CV) strategy is used in the experiments for performance evaluation. Specifically, the whole dataset is first randomly partitioned into five subsets (with approximately equal sample size). We then iteratively treat each subset as the test set, while the remaining four subsets are combined to construct the training set. An inner CV strategy is further applied on each training set for parameter selection. The final results are reported on the test set.

Two tasks are included in the proposed method, i.e., classification for severity assessment, and 2) segmentation for lung lobe. For performance evaluation, two sets of metrics are used in these two tasks, with the details given below.

1) *Metrics for Classification*: We use five commonly used metrics to evaluate the classification performance achieved by different methods in the severity assessment task, i.e., Accuracy, Precision, Recall, F1 Score, and the area under the receiver operating characteristic curve (AUC).

$$Accuracy = \frac{TP + TN}{TP + TN + FP + FN}, \quad (6)$$

$$Precision = \frac{TP}{TP + FP}, \quad Recall = \frac{TP}{TP + FN}, \quad (7)$$

$$F1\ Score = \frac{2 \times Precision \times Recall}{Precision + Recall}. \quad (8)$$

where TP, TN, FP and FN denote true positive, true negative, false positive and false negative, respectively.

2) *Metrics for Segmentation*: We use three metrics, i.e., Dice Similarity Coefficient (DSC), Positive Predict Value (PPV) and Sensitivity (SEN), to evaluate the segmentation performance of different methods, with the definitions given below.

$$DSC = \frac{2\|V_{gt} \cap V_{seg}\|}{\|V_{gt}\| + \|V_{seg}\|}, \quad (9)$$

$$PPV = \frac{\|V_{gt} \cap V_{seg}\|}{\|V_{seg}\|}, \quad SEN = \frac{\|V_{gt} \cap V_{seg}\|}{\|V_{gt}\|}. \quad (10)$$

where V_{gt} and V_{seg} represent the ground-truth and predicted segmentation maps for each scan, respectively.

D. Comparison with State-of-the-art Methods

1) *Results of Severity Assessment*: We first report the performance of six different methods in the task of severity assessment for COVID-19 patients, with the results shown in Table II. As can be seen, four deep learning based methods usually outperforms two hand-crafted feature based methods in most cases. While three MIL methods (i.e., [32], Cls. Only, and M²UNet) yield satisfied performance, the proposed M²UNet achieves the best results (e.g., the accuracy of 98.5% and F1 Score of 99.1%). The receiver operating characteristic (ROC) curves of six competing methods are illustrated in Fig. 6. Note that this ROC curve is plotted based on the results on one fold testing data, which is slightly different from the average performance on five folds in Table II. Table II and Fig. 6 clearly suggest that our M²UNet generate the overall best performance in the task of severity assessment of COVID-19 patients based on chest CT images.

2) *Results of Lung Lobe Segmentation*: We then report the results of lung lobe segmentation achieved by four different methods in Table III. Comparing Seg. Only with the conventional U-Net, the former dramatically reducing the parameter from 131.71MB to 14.37MB. As a consequence, the performance in terms of DSC and PPV is also decreased by 1.7% and 4.9%, respectively. By using multi-task learning, M²Net improves the performance, from 0.759 to 0.785 in terms of DSC, which also outperform the performance of conventional U-Net, with a decreasing of parameters, from 131.71 to 15.32. The proposed M²UNet also achieves a slightly higher performance compared with U-Net++.

The visualization of segmentation results achieved by three different methods on two subjects are shown in Fig. 5. From this figure, we can see that M²UNet generates the overall best segmentation masks, while U-Net and U-Net++ usually yield under-segmentation results on these cases. These results further show the advantage of our M²UNet.

E. Ablation Study

We further evaluate the influence of two major strategies used in our M²UNet, i.e., 1) the hierarchical MIL strategy for classification, and 2) the multi-task learning strategy for joint severity assessment and lung lobe segmentation.

1) *Influence of Hierarchical MIL Strategy*: To evaluate the effectiveness of the hierarchical MIL strategy, we compare the variant of the proposed M²UNet (i.e., Cls. Only without the segmentation subnetwork) with a non-MIL method (i.e., ResNet50+Max) and a one-stage MIL method (i.e., Gated Att. MIL [32]). The classification results of these three methods in the task of severity assessment are reported in Table IV. As shown in Table IV, two MIL methods (i.e., Gated Att. MIL and Cls. Only) can generate more accurate decisions under the weakly supervised setting, compared with the non-MIL method ResNet50+Max. Besides, our hierarchical MIL strategy can further boost the classification performance compared to the conventional one-stage MIL strategy. For instance, our Cls. Only method achieves an F1 Score of 0.938, which is higher than that (i.e., 0.906) yielded by Gated Att. MIL with a one-stage MIL strategy. These results suggest the effectiveness of the proposed hierarchical MIL strategy.

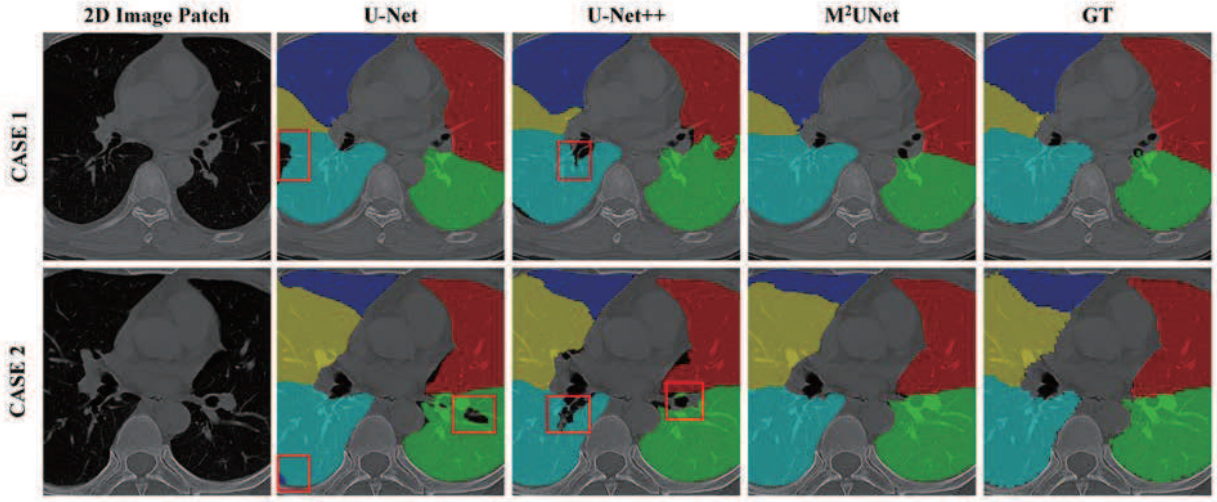


Fig. 5. The visualization of lung lobe segmentation results for different methods on two typical cases. GT denotes the ground-truth masks. The under-segmentation regions are denoted by red boxes.

TABLE IV

EVALUATION OF THE PROPOSED HIERARCHICAL MULTI-INSTANCE LEARNING STRATEGY.

Method	Accuracy	Precision	Recall	F1 Score	AUC
ResNet50+Max [31]	0.924 ± 0.497	0.856 ± 0.154	0.793 ± 0.106	0.816 ± 0.120	0.803 ± 0.090
Gated Att. MIL [32]	0.955 ± 0.015	0.879 ± 0.054	0.946 ± 0.019	0.906 ± 0.037	0.973 ± 0.024
Cls. Only (Ours)	0.969 ± 0.023	0.928 ± 0.073	0.958 ± 0.031	0.938 ± 0.045	0.980 ± 0.013

TABLE V

EVALUATION OF THE PROPOSED MULTI-TASK LEARNING STRATEGY FOR SEVERITY ASSESSMENT.

Method	Accuracy	Precision	Recall	F1 Score	AUC
Cls. Only	0.969 ± 0.023	0.928 ± 0.073	0.958 ± 0.031	0.938 ± 0.045	0.980 ± 0.013
M²UNet	0.985 ± 0.005	0.975 ± 0.022	0.952 ± 0.011	0.963 ± 0.011	0.991 ± 0.010

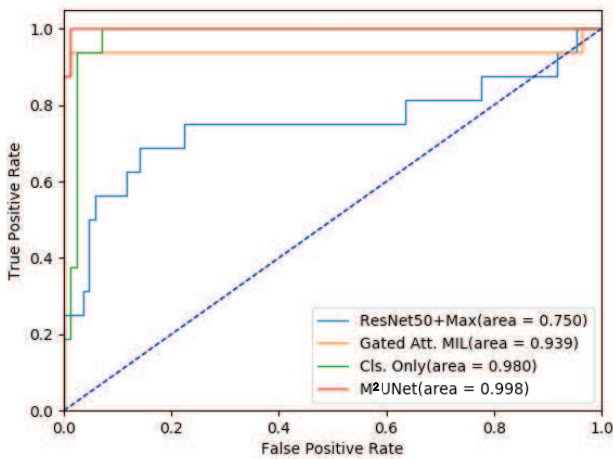


Fig. 6. The receiver operating characteristic (ROC) curves achieved by four different methods in the task of severity assessment.

2) *Influence of Multi-task Learning Strategy*: Our M²UNet can jointly learn the segmentation task and the classification task in a multi-task learning manner. Here, we also investigate

the influence of such a multi-task learning paradigm, by comparing M²UNet with its two single-task variants, i.e., ‘Cls. Only’ for classification and ‘Seg. Only’ for segmentation. The performance comparison in two tasks for severity assessment and lung lobe segmentation are reported in Table V and Table VI, respectively. Table V suggests that, compared with Cls. Only, the multi-task learning paradigm used in M²UNet helps to improve the classification Accuracy by 1.6%, while increasing the F1 Score by 2.5%. As can be observed from Table VI, although M²UNet is not specifically designed for lung lobe segmentation, it still improves the overall segmentation performance in terms of three metrics, compared with its single-task variant (i.e., Seg. Only). This implies that the proposed multi-task learning strategy is useful in boosting the learning performance of both tasks of severity assessment and lung lobe segmentation.

V. CONCLUSION AND FUTURE WORK

In this paper, we propose a synergistic learning framework for automated severity assessment and lung segmentation of COVID-19 in 3D chest CT images. In this framework, we first

TABLE VI

EVALUATION OF THE PROPOSED MULTI-TASK LEARNING STRATEGY FOR LUNG LOBE SEGMENTATION.

Method	DSC	SEN	PPV
Seg. Only	0.759 ± 0.055	0.756 ± 0.064	0.785 ± 0.045
M ² UNet	0.785 ± 0.058	0.783 ± 0.059	0.799 ± 0.051

represent each input image by a bag to deal with the challenging problem that only a few infected regions in the CT image are related to the severity assessment. We further develop a multi-task multi-instance deep network (called M²UNet) to assess the severity of COVID-19 patients and segment the lung lobe simultaneously, where the context information provided by segmentation can be employed to boost the performance of severity assessment. A hierarchical multi-instance learning strategy is also proposed in M²UNet for severity assessment. Experimental results on a real COVID-19 CT image dataset demonstrate that our method achieves promising results in severity assessment of COVID-19 patients, compared with several state-of-the-art methods.

In the current work, the severity assessment of COVID-19 only relies on static data (i.e., chest CT images at one time point), without considering the longitudinal imaging biomarkers. It is interesting to perform longitudinal study to investigate the disease progression, which is one of our future work. Since annotations for lung lobe in 3D CT images are usually tedious and error-prone, only a small number of subjects in our dataset have ground-truth segmentation. Therefore, it is highly desired to develop automated or even semi-automated image annotation methods, which will also be studied in the future.

REFERENCES

- [1] Worldometers, "COVID-19 CORONAVIRUS PANDEMIC," <https://www.worldometers.info/coronavirus/>, 2020, [Online].
- [2] J. Chen, L. Wu, J. Zhang, L. Zhang, D. Gong, Y. Zhao, S. Hu, Y. Wang, X. Hu, B. Zheng *et al.*, "Deep learning-based model for detecting 2019 novel coronavirus pneumonia on high-resolution computed tomography: A prospective study," *medRxiv*, 2020.
- [3] Y. Song, S. Zheng, L. Li, X. Zhang, X. Zhang, Z. Huang, J. Chen, H. Zhao, Y. Jie, R. Wang *et al.*, "Deep learning enables accurate diagnosis of novel coronavirus (COVID-19) with CT images," *medRxiv*, 2020.
- [4] Z. Tang, W. Zhao, X. Xie, Z. Zhong, F. Shi, J. Liu, and D. Shen, "Severity assessment of coronavirus disease 2019 (COVID-19) using quantitative features from chest CT images," *arXiv preprint arXiv:2003.11988*, 2020.
- [5] F. Shan, Y. Gao, J. Wang, W. Shi, N. Shi, M. Han, Z. Xue, D. Shen, and Y. Shi, "Lung infection quantification of COVID-19 in CT images with deep learning," *arXiv preprint arXiv:2003.04655*, 2020.
- [6] S. Jin, B. Wang, H. Xu, C. Luo, L. Wei, W. Zhao, X. Hou, W. Ma, Z. Xu, Z. Zheng *et al.*, "AI-assisted CT imaging analysis for COVID-19 screening: Building and deploying a medical AI system in four weeks," *medRxiv*, 2020.
- [7] X. Qi, Z. Jiang, Q. Yu, C. Shao, H. Zhang, H. Yue, B. Ma, Y. Wang, C. Liu, X. Meng *et al.*, "Machine learning-based CT radiomics model for predicting hospital stay in patients with pneumonia associated with SARS-CoV-2 infection: A multicenter study," *medRxiv*, 2020.
- [8] F. Shi, J. Wang, J. Shi, Z. Wu, Q. Wang, Z. Tang, K. He, Y. Shi, and D. Shen, "Review of artificial intelligence techniques in imaging data acquisition, segmentation and diagnosis for COVID-19," *CoRR*, vol. abs/2004.02731, 2020. [Online]. Available: <https://arxiv.org/abs/2004.02731>
- [9] R. Verity, L. C. Okell, I. Dorigatti, P. Winskill, C. Whittaker, N. Imai, G. Cuomo-Dannenburg, H. Thompson, P. G. Walker, H. Fu *et al.*, "Estimates of the severity of coronavirus disease 2019: a model-based analysis," *The Lancet Infectious Diseases*, 2020.
- [10] B. Zhou, A. Khosla, A. Lapedriza, A. Oliva, and A. Torralba, "Learning deep features for discriminative localization," in *Proceedings of the IEEE conference on computer vision and pattern recognition*, 2016, pp. 2921–2929.
- [11] O. Ronneberger, P. Fischer, and T. Brox, "U-net: Convolutional networks for biomedical image segmentation," in *International Conference on Medical Image Computing and Computer-Assisted Intervention*. Springer, 2015, pp. 234–241.
- [12] C. Zheng, X. Deng, Q. Fu, Q. Zhou, J. Feng, H. Ma, W. Liu, and X. Wang, "Deep learning-based detection for COVID-19 from chest CT using weak label," *medRxiv*, 2020.
- [13] Y. Cao, Z. Xu, J. Feng, C. Jin, X. Han, H. Wu, and H. Shi, "Longitudinal assessment of COVID-19 using a deep learning-based quantitative CT pipeline: Illustration of two cases," *Radiology: Cardiothoracic Imaging*, vol. 2, no. 2, p. e200082, 2020.
- [14] L. Huang, R. Han, T. Ai, P. Yu, H. Kang, Q. Tao, and L. Xia, "Serial quantitative chest CT assessment of COVID-19: Deep-learning approach," *Radiology: Cardiothoracic Imaging*, vol. 2, no. 2, p. e200075, 2020.
- [15] Z. Zhou, M. M. R. Siddiquee, N. Tajbakhsh, and J. Liang, "Unet++: A nested u-net architecture for medical image segmentation," in *Deep Learning in Medical Image Analysis and Multimodal Learning for Clinical Decision Support*. Springer, 2018, pp. 3–11.
- [16] F. Milletari, N. Navab, and S.-A. Ahmadi, "V-net: Fully convolutional neural networks for volumetric medical image segmentation," in *2016 Fourth International Conference on 3D Vision (3DV)*. IEEE, 2016, pp. 565–571.
- [17] T. G. Dietterich, R. H. Lathrop, and T. Lozano-Pérez, "Solving the multiple instance problem with axis-parallel rectangles," *Artificial Intelligence*, vol. 89, no. 1-2, pp. 31–71, 1997.
- [18] K. Xu, J. Ba, R. Kiros, K. Cho, A. Courville, R. Salakhudinov, R. Zemel, and Y. Bengio, "Show, attend and tell: Neural image caption generation with visual attention," in *International Conference on Machine Learning*, 2015, pp. 2048–2057.
- [19] M. Liu, J. Zhang, E. Adeli, and D. Shen, "Joint classification and regression via deep multi-task multi-channel learning for Alzheimer's disease diagnosis," *IEEE Transactions on Biomedical Engineering*, vol. 66, no. 5, pp. 1195–1206, 2018.
- [20] M. Oquab, L. Bottou, I. Laptev, J. Sivic *et al.*, "Weakly supervised object recognition with convolutional neural networks," in *NIPS*, 2014, pp. 1545–5963.
- [21] J. Feng and Z.-H. Zhou, "Deep miml network," in *Thirty-First AAAI Conference on Artificial Intelligence*, 2017.
- [22] M. Sun, T. X. Han, M.-C. Liu, and A. Khodayari-Rostamabad, "Multiple instance learning convolutional neural networks for object recognition," in *2016 23rd International Conference on Pattern Recognition (ICPR)*. IEEE, 2016, pp. 3270–3275.
- [23] J. Wu, Y. Yu, C. Huang, and K. Yu, "Deep multiple instance learning for image classification and auto-annotation," in *Proceedings of the IEEE Conference on Computer Vision and Pattern Recognition*, 2015, pp. 3460–3469.
- [24] T. Tong, R. Wolz, Q. Gao, R. Guerrero, J. V. Hajnal, and D. Rueckert, "Multiple instance learning for classification of dementia in brain MRI," *Medical Image Analysis*, vol. 18, no. 5, pp. 808–818, 2014.
- [25] Y. Xu, J.-Y. Zhu, I. Eric, C. Chang, M. Lai, and Z. Tu, "Weakly supervised histopathology cancer image segmentation and classification," *Medical Image Analysis*, vol. 18, no. 3, pp. 591–604, 2014.
- [26] Z. Yan, Y. Zhan, Z. Peng, S. Liao, Y. Shinagawa, S. Zhang, D. N. Metaxas, and X. S. Zhou, "Multi-instance deep learning: Discover discriminative local anatomies for bodypart recognition," *IEEE Transactions on Medical Imaging*, vol. 35, no. 5, pp. 1332–1343, 2016.
- [27] M. Liu, J. Zhang, E. Adeli, and D. Shen, "Landmark-based deep multi-instance learning for brain disease diagnosis," *Medical Image Analysis*, vol. 43, pp. 157–168, 2018.
- [28] K. He, X. Cao, Y. Shi, D. Nie, Y. Gao, and D. Shen, "Pelvic organ segmentation using distinctive curve guided fully convolutional networks," *IEEE Transactions on Medical Imaging*, vol. 38, no. 2, pp. 585–595, 2018.
- [29] C. Lian, M. Liu, J. Zhang, and D. Shen, "Hierarchical fully convolutional network for joint atrophy localization and Alzheimer's disease diagnosis using structural MRI," *IEEE Transactions on Pattern Analysis and Machine Intelligence*, 2018.

-
- [30] S. Bakas, M. Reyes, A. Jakab, S. Bauer, M. Rempfler, A. Crimi, R. T. Shinohara, C. Berger, S. M. Ha, M. Rozycki *et al.*, “Identifying the best machine learning algorithms for brain tumor segmentation, progression assessment, and overall survival prediction in the BRATS challenge,” *arXiv preprint arXiv:1811.02629*, 2018.
 - [31] C. Szegedy, S. Ioffe, V. Vanhoucke, and A. A. Alemi, “Inception-v4, inception-resnet and the impact of residual connections on learning,” in *Thirty-first AAAI Conference on Artificial Intelligence*, 2017.
 - [32] M. Ilse, J. M. Tomczak, and M. Welling, “Attention-based deep multiple instance learning,” *CoRR*, vol. abs/1802.04712, 2018. [Online]. Available: <http://arxiv.org/abs/1802.04712>
 - [33] R. Yang, X. Li, H. Liu, Y. Zhen, X. Zhang, Q. Xiong, Y. Luo, C. Gao, and W. Zeng, “Chest CT severity score: An imaging tool for assessing severe COVID-19,” *Radiology: Cardiothoracic Imaging*, vol. 2, no. 2, p. e200047, 2020.

Synergistic Learning of Lung Lobe Segmentation and Hierarchical Multi-Instance Classification for Automated Severity Assessment of COVID-19 in CT Images – *Supplementary Materials*

arXiv:2005.03832v1 [eess.IV] 8 May 2020

Besides the experimental results in the main text, we further analyze the influence of parameters on the performance of the proposed M²UNet, with the details given below.

I. INFLUENCE OF WEIGH PARAMETER

We evaluate the influence of the hyper-parameter λ . The boxplot for the margin of prediction and ground-truth labels is shown in Fig. 1, where the margin is calculated by $|p - l|$, p denotes the prediction score and l denotes the label. The margin below 0.5 indicates that the prediction is correct. As shown in this figure, the task weight λ affects the classification performance of the model, and the proposed M²UNet performs best with $\lambda = 0.01$.

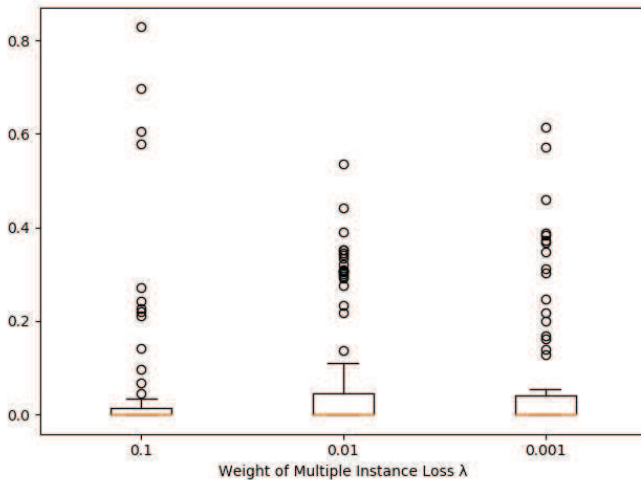


Fig. 1. Boxplot for the margin of prediction and label with respect to different weight λ for multiple instance loss. The margin larger than 0.5 indicates the wrong prediction.

II. INFLUENCE OF LEARNING RATE

We further investigate the influence of the learning rate on the performance of M²UNet, with the results given in Tables I-II. As suggested by the table, the performance of M²UNet for both classification and segmentation tasks are affected by

TABLE I

PERFORMANCE COMPARISON FOR SEGMENTATION WITH RESPECT TO DIFFERENT LEARNING RATE.

Learning rate	DSC	SEN	PPV
0.1	0.783	0.772	0.789
0.01	0.785	0.783	0.799
0.001	0.734	0.705	0.754

TABLE II

PERFORMANCE COMPARISON FOR SEVERITY PREDICTION WITH RESPECT TO DIFFERENT LEARNING RATE.

Learning rate	Accurate	Precision	Recall	F1 Score
0.1	0.946	0.833	0.970	0.885
0.01	0.985	0.975	0.952	0.963
0.001	0.960	0.881	0.922	0.900

different learning rates. The proposed method achieves the best performance for both classification and segmentation tasks with the learning rate of 0.01. Another observation is that the performance of the network is unstable with a large learning rate (i.e., 0.1), and the gap between precision and recall is large, with 0.833 in terms of precision and 0.970 in terms of recall. The performance of the network is stable with a small learning rate (i.e., 0.001), with precision of 0.881 and recall of 0.922. However, it cannot achieve the best performance, compared with the network trained by the learning rate of 0.01.